

PraFFL: A Preference-Aware Scheme in Fair Federated Learning

Rongguang Ye
yerg2023@mail.sustech.edu.cn
Southern University of Science and
Technology
Shenzhen, China

Wei-Bin Kou
wbkou@connect.hku.hk
The University of Hong Kong
Hong Kong, China

Ming Tang*
tangm3@sustech.edu.cn
Southern University of Science and
Technology
Shenzhen, China

Abstract

Fairness in federated learning has emerged as a critical concern, aiming to develop an unbiased model for any special group (e.g., male or female) of sensitive features. However, there is a trade-off between model performance and fairness, i.e., improving model fairness will decrease model performance. Existing approaches have characterized such a trade-off by introducing hyperparameters to quantify client's preferences for model fairness and model performance. Nevertheless, these approaches are limited to scenarios where each client has only a single pre-defined preference, and fail to work in practical systems where each client generally have multiple preferences. The key challenge is to design a method that allows the model to adapt to diverse preferences of each client in real time. To this end, we propose a Preference-aware scheme in Fair Federated Learning paradigm (called PraFFL) to generate preference-wise model in real time. PraFFL can adaptively adjust the model based on each client's preferences to meet their needs. We theoretically prove that PraFFL can offer the optimal model tailored to an arbitrary preference of each client, and show its linear convergence. Experimental results show that our proposed PraFFL outperforms five fair federated learning algorithms in terms of the model's capability of adapting to clients' different preferences.

CCS Concepts

• **Computing methodologies** → **Distributed artificial intelligence**.

Keywords

Fairness, Federated Learning, Trade-Off, Preference-Aware, Model Adaptation, Theoretical Guarantee

ACM Reference Format:

Rongguang Ye, Wei-Bin Kou, and Ming Tang. 2018. PraFFL: A Preference-Aware Scheme in Fair Federated Learning. In *Proceedings of Make sure to enter the correct conference title from your rights confirmation email (Conference acronym 'XX)*. ACM, New York, NY, USA, 14 pages. <https://doi.org/XXXXXX.XXXXXXX>

*Corresponding author.

Permission to make digital or hard copies of all or part of this work for personal or classroom use is granted without fee provided that copies are not made or distributed for profit or commercial advantage and that copies bear this notice and the full citation on the first page. Copyrights for components of this work owned by others than the author(s) must be honored. Abstracting with credit is permitted. To copy otherwise, or republish, to post on servers or to redistribute to lists, requires prior specific permission and/or a fee. Request permissions from permissions@acm.org.
Conference acronym 'XX, June 03–05, 2018, Woodstock, NY

© 2018 Copyright held by the owner/author(s). Publication rights licensed to ACM.
ACM ISBN 978-1-4503-XXXX-X/18/06
<https://doi.org/XXXXXX.XXXXXXX>

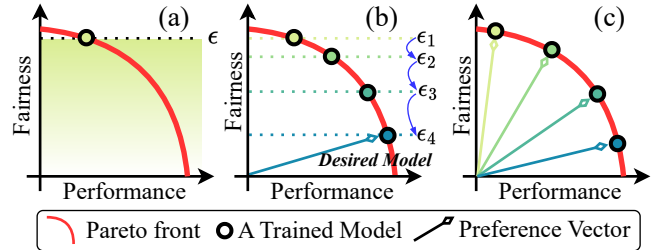


Figure 1: The model trained under different settings. Pareto front is the optimal performance-fairness curve (usually not known in advance). (a) The model is trained under a specific fair budget ϵ . (b) The process of adjusting the constraint level to meet a specific preference (from ϵ_1 to ϵ_4). (c) The model is trained under our proposed method, aiming at obtaining a preference-aware model.

1 Introduction

Federated learning (FL) is a distributed machine learning method that learns from multiple client data sources [24, 35], where a global model is trained cooperatively among clients without sharing data. Since the global model learns from multiple data sources, it has a stronger generalization ability across multiple clients than separately training model for each client [38]. However, a key concern in FL is to ensure the trained model being unbiased towards any particular groups (e.g., special races) of sensitive features [15, 19, 30]. This implies that a fair model needs to treat different groups equally, such that the model's prediction result is identical across different groups.

Fair FL was proposed to improve the fairness of the model [1, 10, 29, 40], where the fairness of the model is usually defined as the differences in predictions across different groups. Specifically, the smaller prediction differences among different groups, the better fairness the model has. Unfortunately, many studies [8, 14, 37] stated that improving model fairness and model performance in FL is a trade-off issue, i.e., model fairness and model performance cannot be improved simultaneously. Some existing works characterized the trade-off using hyperparameters. For example, LFT+Fedavg [1] takes the fairness of the model as a constraint (see Fig. 1(a)). FairFed [10] introduces a hyperparameter as a fair budget to adjust the aggregation weights when clients communicate models with the server. FAIR-FATE [33] takes the linear combination of model performance and model fairness as the optimization objective. However, most of aforementioned works have two main limitations. First, their determined models may not satisfy a client's given preference over model fairness and model performance. Specifically, those budget-based approaches (e.g., LFT+FedAvg and FairFed) aim to match only fairness but to ignore performance. For example, Fig.

Table 1: Strengths of PraFFL against other fair FL methods in case of N preferences.

Method	Time Complexity	Real-Time Adaption	Preference Awareness
LFT+Ensemble [40]	$O(N)$	✗	✗
LFT+Fedavg [20]	$O(N)$	✗	✗
Agnosticfair [8]	$O(N)$	✗	✗
FairFed [10]	$O(N)$	✗	✗
FedFB [40]	$O(N)$	✗	✗
PraFFL (Ours)	$O(1)$	✓	✓

1(b) depicts that LFT+Fedavg needs to repeatedly train the model after adjusting fair budget ϵ until the desired model is obtained. Those multi-objective-based approaches (e.g., FAIR-FATE) can obtain the desired model only when the shape of the optimal performance-fairness curve (also called Pareto front) is convex [3], while such a convexity is not necessarily satisfied in FL scenario. Second, the aforementioned approaches (e.g., [1, 10, 33]) may not be applicable to the scenario where each client has multiple preferences. A practical example is to take the social platform TikTok as a client to meet diverse preferences from billions of users [16]. In particular, the users expect the model to recommend high-quality videos that align with their interests, i.e., these users prioritize model performance. In contrast, some other users seek unbiased recommendations towards/against any particular racial group, i.e., these users prioritize model fairness. For those aforementioned works (e.g., [1, 10, 29]), when each client has different requirements (i.e. preferences), their model needs to be retrained multiple times to adapt each requirement. Thus, their time complexity grows linearly with the number of preferences. Table 1 shows that the time complexity of other methods to satisfy a client’s N preferences is $O(N)$ and does not support real-time model adaptation based on client’s preferences. Inspired by this, we aim to answer the following research questions:

How can the model (i) effectively align with each client’s specific preference and (ii) be adaptively adjusted in real time based on each client’s diverse preferences?

These problems involve three technical challenges: (I) establishing the connection between the two objectives (performance and fairness) and the client’s preference; (II) alleviating the impact of data heterogeneity; and (III) preventing the privacy leakage of client preferences. To this end, we propose a **Preference-Aware** scheme in **Fair Federated Learning (PraFFL)**. Fig. 1(c) shows that our proposed PraFFL can accurately learn a mapping from the preference vector to a trade-off point between model performance and model fairness, through which PraFFL enables the model to connect its fairness and performance with the corresponding preference vector. In PraFFL, we include a personalized FL method to alleviate the impact of data heterogeneity. Meanwhile, we introduce a hyper-network that can decouple each client’s preference information from other clients and the server to protect the privacy of clients. Our proposed PraFFL can provide the preference-wise model to each client. In other words, once the model is trained by PraFFL, it allows the model to adapt to each client’s preferences during the inference phase. In addition, PraFFL is theoretically proven to obtain the Pareto front within one training. In summary, as demonstra

in Table 1, our proposed PraFFL can achieve the time complexity of $O(1)$, and can generate the preference-wise model that is adaptive according to the client’s preference.

The main contributions of this paper are highlighted as follows:

- We present a preference learning framework, which enables the model to adapt to different preferences of each client.
- We propose a PraFFL scheme to further address the three technical challenges while allowing the model to adapt to arbitrary preferences of each client.
- We theoretically prove that PraFFL can linearly converge to optimal model that meets each client’s preference, and can learn the Pareto front on each client’s dataset.
- Numerical experiments validate that our proposed PraFFL outperforms other baselines on four datasets in terms of the model’s capability in adapting to clients’ different preferences.

2 Related Work

There are two types of fairness in fair FL: client-based fairness [22, 23, 27, 36] and group-based fairness [7, 27, 39]. The purpose of client-based fairness is to reduce the variance of model performance across all clients while maintaining the performance of these models. Our work mainly discusses group-based fairness, in which each client has some sensitive features (e.g., gender and race). The goal of group-based fairness is to avoid discrimination against sensitive features [18, 32, 41]. Many recent studies [8, 10, 31] investigated how to achieve group fairness in FL. For example, an adaptive FairBatch debiasing algorithm [32] was proposed under the FL framework, in which the optimization problem of each client is a bi-level optimization problem of model fairness and sampling probability for different groups. FedVal [25] is another global reweighting strategy, where the client’s aggregation weight depends on the fairness budget of the model in the validation set. However, previous studies have shown that improving model performance and model fairness is a trade-off problem [10, 31, 33, 40]. To control the trade-off between model performance and fairness, the most common approach is to treat fairness as a constraint in optimizing each client’s model [8, 13, 42]. Specially, FAIR-FATE [33] introduces a weight coefficient to linearly combine fairness and model performance as the final optimization goal. Furthermore, Fairfed [10] uses the FairBatch debiasing algorithm [32] to ensure the model fairness in the model optimization stage, and designs a reweight method in the aggregation stage to control the trade-off of the model for performance and fairness. However, most of the above methods can only obtain a model corresponding to one of the client’s preferences. It is challenging for the aforementioned methods to meet diverse client preferences.

3 Problem Formulation

3.1 Multi-Objective Learning

Let $\mathbf{b} \in \mathcal{B}$ and $y \in \mathcal{Y}$ denote the non-sensitive features and labels of dataset \mathcal{D} , respectively. $a \in \mathcal{A}$ represents the sensitive feature where a supports the inclusion of multi-dimensional sensitive information, for example, young man for both age and gender dimensions. The feature vector can be further expressed as $\mathbf{x} \triangleq (a, \mathbf{b}) \in \mathcal{X}$. According to [4, 40], we consider a binary classification problem

(i.e., $y \in \mathcal{Y} \triangleq \{0, 1\}$, where $y = 1$ indicates positive class) and multi-group sensitive feature (i.e., $a \in \mathcal{A} \triangleq \{0, \dots, m\}$). Now, we introduce two objectives in fair FL, i.e., model performance and model fairness.

Model Performance. Let $\theta : \mathcal{X} \rightarrow \mathcal{Y}$ be a classifier. Usually, the cross-entropy loss function is used to quantify the model performance in the classification problem, and it is defined as follow:

$$\mathcal{L}_1(x, y, \theta) = -[y \log(\theta(x)) + (1 - y) \log(1 - \theta(x))], \quad (1)$$

where $\theta(x)$ represents probability of predicting a data sampled with feature x belongs to the positive class.

Model Fairness. A widely adopted criterion for assessing classifier fairness is *DP disparity* [11]. Let \hat{y} represent the the label predicted by the classifier based on feature x . DP disparity quantifies the maximum difference in expectation of the classifier θ that predicts a data sample to be in positive class across different sensitive groups

$$\max_{j \in \mathcal{A}} |\mathbb{E}_{(x,y) \sim \mathcal{D}_k} [\hat{y} = 1 | a = j] - \mathbb{E}_{(x,y) \sim \mathcal{D}_k} [\hat{y} = 1]|. \quad (2)$$

Due to the discontinuity of Eq. (2), model fairness is usually characterized by the following proxy loss function [40]

$$\mathcal{L}_2(x, y, \theta) = [(a - \bar{a})(\theta(x) - \bar{\theta}(x))]^2, \quad (3)$$

where \bar{a} and $\bar{\theta}(x)$ represent the average values of a and $\theta(x)$ over \mathcal{D} , respectively. \mathcal{L}_2 quantifies the correlation between sensitive features and the model predictions. A higher value of \mathcal{L}_2 suggests that sensitive features are more strongly correlated with the model's predicted probabilities, indicating a lower fairness.

Then, we convert the fair FL into a multi-objective problem to solve, which can be expressed as follows:

$$\min_{\theta \in \Theta} \mathcal{L}(x, y, \theta) = (\mathcal{L}_1(x, y, \theta), \mathcal{L}_2(x, y, \theta)), \quad (4)$$

where $\mathcal{L}(x, y, \theta) : \mathcal{X} \times \mathcal{Y} \times \Theta \rightarrow \mathbb{R}_{\geq 0}^2$ is a two-dimensional objective vector. For presentation simplicity, in the rest of this paper, we use the terms "solution" and "trained model" interchangeably.

Model performance and model fairness are conflicting, and we need to make trade-offs between these two objectives [31, 40]. For ease of notation, let us denote j -th objective as $O_j(\theta) = \mathcal{L}_j(x, y, \theta)$, for all $j \in \{1, 2\}$. We give the following definitions of fair FL in the context of multi-objective optimization [5].

DEFINITION 3.1 (PARETO DOMINANCE). Let $\theta^a, \theta^b \in \Theta$, θ^a is said to dominate θ^b , denoted as $\theta^a < \theta^b$, if and only if $O_i(\theta^a) \leq O_i(\theta^b)$, for all $i \in \{1, 2\}$ and $O_j(\theta^a) < O_j(\theta^b)$, for some $j \in \{1, 2\}$. In addition, θ^a is said to strictly dominate θ^b , denoted as $\theta^a <_{strict} \theta^b$, if and only if $O_i(\theta^a) < O_i(\theta^b)$, for all $i \in \{1, 2\}$.

DEFINITION 3.2 (PARETO OPTIMALITY). $\theta^* \in \Theta$ is Pareto optimal if there does not exist $\hat{\theta} \in \Theta$ such that $\hat{\theta} < \theta^*$. In addition, θ^* is weakly Pareto optimal if there is no $\theta \in \Theta$ such that $\theta <_{strict} \theta^*$.

DEFINITION 3.3 (PARETO SET/FRONT). The set of all Pareto optimal solutions $\mathcal{P}^* \subseteq \Theta$ is called the Pareto set, and its image in the objective space $\mathcal{P}\mathcal{F}^* = \{\mathcal{O}(\theta) \mid \theta \in \mathcal{P}^*\}$ is called the Pareto front.

To evaluate the quality of a solution set, a hypervolume (HV) indicator [12] is commonly used.

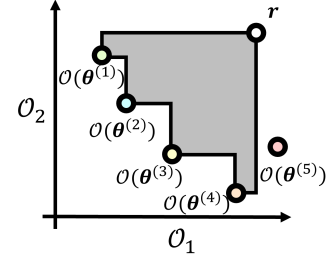


Figure 2: Diagram of hypervolume.

DEFINITION 3.4 (HYPERVOLUME). Let $\hat{\Theta} = \{\theta^{(1)}, \dots, \theta^{(n)}\}$ be a set of objective vectors given solution $\theta^{(i)}$, $i \in [n]$. The hypervolume indicator $\mathcal{H}_r(\hat{\Theta})$ is the two-dimensional Lebesgue measure of the region dominated by $\mathcal{P}^*(\hat{\Theta})$ and bounded by a pre-defined reference point $r \in \mathbb{R}^2$.

Fig. 2 shows the calculation of HV for a set of five solutions, where the gray area represents the HV value. We aim to make the model adapt to client preferences, and to maximize the HV of the Pareto front in the objective space.

3.2 Preference Learning Framework

Inspired by the scalarization method in multi-objective optimization, we introduce preference vector $\lambda \in \Lambda \in \mathbb{R}_{>0}^2$ ($\sum_{i=1}^2 \lambda_i = 1$) and incorporate it into the original multi-objective optimization problem (Eq. (4)) to characterize clients' preference information. In particular, we consider a generalized setting [21] where each client k aims to obtain its own model θ_k . This setting can generalize the conventional FL case where clients aim to learn an identical global model. To enable the model to adapt to each client's individual preference, we concatenate (\oplus) the input x with the preference vector λ as joint features for training each client's local model $\theta_k : \mathcal{X} \oplus \Lambda \rightarrow \mathcal{Y}$. By considering the preference vector in FL system, Eq. (4) can be transformed to

$$\min_{(\theta_1, \dots, \theta_K) \in \Theta_K} \frac{1}{K} \sum_{k \in [K]} \mathbb{E}_{\lambda \sim \Lambda} \mathbb{E}_{(x,y) \sim \mathcal{D}_k} \lambda \cdot \mathcal{L}((x \oplus \lambda), y, \theta_k), \quad (5)$$

where Θ_K is the feasible space of K models. \mathcal{D}_k represents the dataset of client k . The system aims to provide models tailored to any preference. Hence, the system must be trained on the expectation of preference distribution Λ to encompass all potential preferences. In practice, the distribution Λ can be set to a uniform distribution when there is no prior knowledge of clients. Once the model θ_k ($k \in [K]$) is optimized, the prediction results of each client's dataset will be determined by each client's given preference in the inference phase. Pareto front can be generated by examining the models of all possible preference vectors in the inference phase (i.e., one preference generates one Pareto optimal solution).

Although our proposed preference learning framework (Eq. (5)) takes client preferences into account, there are three difficulties in obtaining high-quality Pareto front by Eq. (5):

- (I) We have no prior knowledge of the Pareto front shape. According to [3], a weight-sum function in Eq. (5) only works when the Pareto front is convex. Eq. (5) cannot guarantee Pareto optimal solution is in the direction of preference vector when the Pareto front is concave (illustrated in Fig. 3(a)).

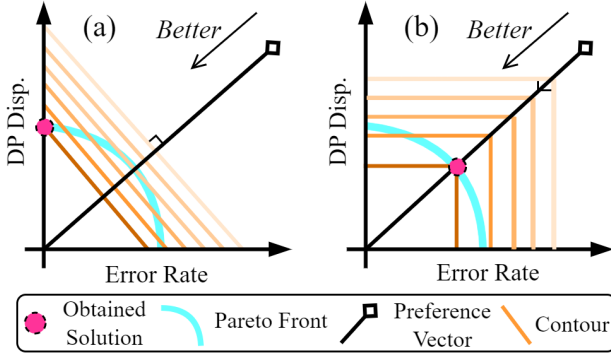


Figure 3: The solution obtained by different optimization functions. (a): The weighted-sum function (Eq. (5)). (b): The weighted Tchebycheff function (Eq. (7)).

- (II) The data distribution among different clients is heterogeneous, that is, their Pareto fronts are also different (depending on each client’s data distribution).
- (III) Optimizing the system via Eq. (5) may leak preference information of clients (e.g., data reconstruction attack [34]) because preference vectors are used as input data.

4 The Proposed Method: PraFFL

In this section, we propose a preference-aware scheme in fair FL (PraFFL) to further address three difficulties in solving Eq. (5). Section 4.1 presents a preference alignment approach to address difficulty (I). Moreover, Section 4.2 introduces a personalized FL based on preferences to solve difficulty (II). Furthermore, we propose to use a hypernetwork to consider preferences in Section 4.3, which protects the clients’ preference privacy (addressing difficulty (III)). In addition, Section 4.4 summarizes the algorithm details of PraFFL scheme.

4.1 Alignment of Model with Preference

It is difficult to provide a model whose performance and fairness fall in the direction of the client’s corresponding preference vector. To obtain a Pareto optimal solution in the direction of any given preference vector, we introduce a weighted Tchebycheff function [26] as the optimization function for each client as follows:

$$\min_{\theta_k} g_t(\mathbf{x} \oplus \lambda, y, \theta_k | \lambda) = \min_{\theta_k} \max_{i \in \{1,2\}} \left\{ \frac{\mathcal{L}_i(\mathbf{x} \oplus \lambda, y, \theta_k)}{\lambda_i} \right\}. \quad (6)$$

We can obtain the following promising property of problem (6).

LEMMA 4.1 (PREFERENCE ALIGNMENT [26]). *Given a preference vector $\lambda > 0$, a solution $\theta_k \in \Theta$ is weakly Pareto optimal to problem 4 if and only if θ_k is an optimal solution to problem (6).*

Lemma 4.1 shows that given a preference vector λ , our method can obtain a weakly Pareto optimal solution for each client if problem (6) is minimal. Then, substituting Eq. (6) into problem (5), the optimization problem in our system can be represented as

$$\min_{(\theta_1, \dots, \theta_K) \in \Theta_K} \frac{1}{K} \sum_{k \in [K]} \mathbb{E}_{\lambda \sim \Lambda} \mathbb{E}_{(\mathbf{x}, y) \sim \mathcal{D}_k} g_t(\mathbf{x} \oplus \lambda, y, \theta_k | \lambda). \quad (7)$$

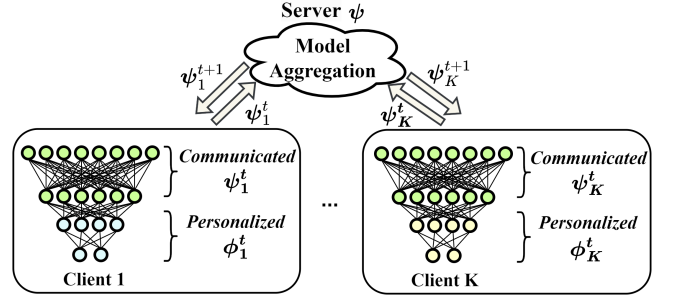


Figure 4: Personalized federated learning framework.

Eq. (7) can optimize each model towards the direction of the preference vector. Fig. 3(a) shows the result obtained by weight-sum function (Eq. (5)), which cannot accurately obtain the model on the preference vector. In Fig. 3(b), the weight Tchebycheff optimization function we introduced can accurately obtain the model on the preference vector if Eq. (7) is minimum. In this way, we can align the model to client’s given preference vector. However, due to the data heterogeneity of clients, problem (7) cannot reach the minimum value, resulting in the failure to meet the condition of Lemma 4.1. In the following subsections, we introduce personalized FL based on hypernetwork mapping, which allows each client to obtain its own optimal model without revealing the privacy of client preferences.

4.2 Personalized FL Based on Preferences

To address difficulty (II) in Section 3, we present a personalized FL framework (see Fig. 4). In this framework, each client’s model is divided into two parts (communicated model and personalized model). The communicated model $\psi : \mathbb{R}^{|\mathcal{X}|} \rightarrow \mathbb{R}^d$ is the part of the model that is shared between clients. d is the dimension of the data after passing through the communicated model. Each client also has a personalized model $\phi_k : \mathbb{R}^d \rightarrow \mathbb{R}^{|\mathcal{Y}|}$. The model of client k is expressed as $\theta_k = (\psi, \phi_k)$. The inclusion of the personalized model can solve difficulty (II) because each client’s personalized model is optimized according to its corresponding data distribution. Thus, by taking into account both the communicated and personalized models, the optimization goal of PraFFL can be transformed into

$$\min_{(\phi_1, \dots, \phi_K) \in \Phi_K} \frac{1}{K} \sum_{k \in [K]} \mathbb{E}_{\lambda \sim \Lambda} \mathbb{E}_{(\mathbf{x}, y) \sim \mathcal{D}_k} g_t(\mathbf{x} \oplus \lambda, y, \theta_k | \lambda), \quad (8a)$$

$$s.t. \psi = \arg \min_{\psi \in \Psi} \frac{1}{K} \sum_{k \in [K]} \mathbb{E}_{\lambda \sim \Lambda} \mathbb{E}_{(\mathbf{x}, y) \sim \mathcal{D}_k} \mathcal{L}_1(\mathbf{x} \oplus \lambda, y, \theta_k). \quad (8b)$$

Our idea is to ensure the performance of the communicated model (Eq. (8b)), and then optimize the personalized model according to the given preferences (Eq. (8a)). As will be seen in later sections, we consider an iterative optimization process. When Eq. (8b) is being optimized, clients collaboratively optimize a global communicated model ψ to minimize cross-entropy loss (performance) over their own datasets. After Eq. (8b) has been optimized, the system optimizes the personalized models of clients, considering the expected model performance and fairness over clients’ preferences. Note that the optimization of communicated model takes into account the preference vector as input. These preference

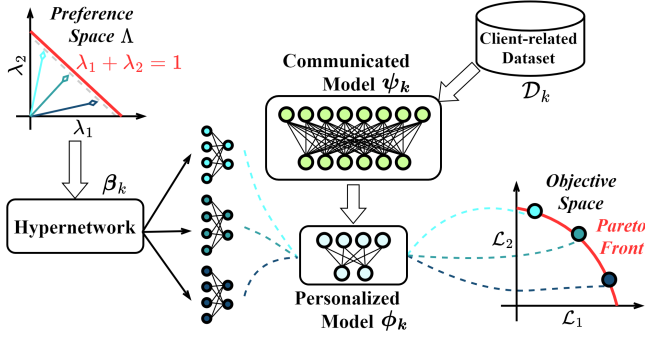


Figure 5: The illustration of hypernetwork inference for client k . Hypernetwork β_k returns the corresponding personalized models to client k based on the preference vectors.

vectors are easily leaked through data reconstruction (difficulty (III)) [17].

4.3 Coupled Preferences with Hypernetwork

To further solve difficulty (III), we introduce a *hypernetwork* to prevent the leakage of the client's preference information. Hypernetwork is deployed on every client. Let $\beta_k : \mathbb{R}^m \rightarrow \mathbb{R}^{|\phi_k|}$ be a hypernetwork, which aims to learn a mapping from the preference vector to the parameters of the personalized model. Given a preference vector λ , the personalized model ϕ_k of client k is determined as follows:

$$\phi_k = \beta_k(\lambda). \quad (9)$$

Based on Eq. (9), client's preference λ are represented as the personalized model via a hypernetwork rather than as part of the joint features (as mentioned in Eq. (5)). Each client k can directly obtain its personalized model by specifying vector λ in Eq. (9). As shown in Fig. 5, if the hypernetwork can be well-trained, then it can generate the personalized model that satisfies the corresponding preference in the inference phase. The model of client k is further expressed as $\theta_k(\lambda) = (\psi, \beta_k(\lambda))$. The optimization problem of our system is transformed into the following

$$\min_{(\beta_1, \dots, \beta_K) \in \mathcal{B}_K} \frac{1}{K} \sum_{k \in [K]} \mathbb{E}_{\lambda \sim \Lambda} \mathbb{E}_{(x, y) \sim \mathcal{D}_k} g_t(x, y, \theta_k(\lambda) | \lambda), \quad (10a)$$

$$\text{s.t. } \psi = \arg \min_{\psi \in \Psi} \frac{1}{K} \sum_{k \in [K]} \mathbb{E}_{\lambda \sim \Lambda} \mathbb{E}_{(x, y) \sim \mathcal{D}_k} \mathcal{L}_1(x, y, \theta_k(\lambda)). \quad (10b)$$

Eq. (10a) aims to learn a mapping relation from preference vector distribution Λ to a set of personalized models. Due to the client's preferences being learned in the hypernetwork, each client's preference information is isolated from other clients. Therefore, hypernetwork can learn each client's preferences while protecting the client's preference information (addressing difficulty (III)). So far, the three difficulties mentioned in Section 3 have been solved.

4.4 PraFFL Algorithm

Now, we propose PraFFL algorithm to solve problem (10), which can generate a preference-wise model for each client while addressing difficulties (I)–(III). Specifically, there are T rounds in total. In each round, a proportion of $p \in (0, 1]$ clients is selected for training, where the set of clients is denoted as \mathcal{S}_t . Then, the communicated

model and the hypernetwork are updated sequentially at each client. Each client k first downloads the global communicated model ψ as its local communicated model ψ_k .

To stabilize the optimization of the communicated model for solving problem (10b), we need to freeze the personalized model when the communicated model is being updated. In particular, personalized model of client k is frozen to $\phi_k = \beta(\tilde{\lambda})$, where $\tilde{\lambda}$ is chosen to be $(\frac{1}{2}, \frac{1}{2})$ so that the personalized model is unbiased towards model performance and fairness when optimizing the local communication model. Client k performs τ_c times of gradient descent algorithm for updating the communicated model at t -th round

$$\psi_k^{t, s+1} = \psi_k^{t, s} - \eta \mathbb{E}_{(x, y) \sim \mathcal{D}_k} \nabla_{\psi_k} \mathcal{L}_1(x, y, \theta_k^{t, s}(\tilde{\lambda})), \quad (11)$$

where $s = 1, \dots, \tau_c$ and η is the learning rate.

After updating the communicated model, each client then optimizes the hypernetwork. The optimization of the hypernetwork aims to enable the personalized models to adapt to different preferences and data heterogeneity. When optimizing the hypernetwork, client k freezes the communicated model as ψ_k^{t, τ_c+1} when optimizing problem (10a). The optimization of the hypernetwork for client k can be expressed as follows:

$$\min_{\beta_k} \mathbb{E}_{\lambda \sim \Lambda} \mathbb{E}_{(x, y) \sim \mathcal{D}_k} g_t(x, y, \theta_k(\lambda)). \quad (12)$$

Eq. (12) is difficult to optimize because there are infinite possible values for λ . We use the Monte Carlo sampling method in stochastic optimization to optimize Eq. (12). Thus, client k performs τ_p

$$\beta_k^{t, j+1} = \beta_k^{t, j} - \eta \mathbb{E}_{(x, y) \sim \mathcal{D}_k} \frac{1}{n_\lambda} \sum_{i=1}^{n_\lambda} \nabla_{\beta_k} g_t(x, y, \theta_k^{t, j}(\lambda^{(i)})), \quad (13)$$

where $j = 1, \dots, \tau_p$, n_λ is the batch size for sampling preference vectors and $\lambda^{(i)}$ is sampled from preference vector distribution Λ . In our work, we set Λ to be a uniform distribution.

Once the communicated model and personalized model of participated clients are updated at t -th round, the participated clients send their communicated models ψ_k ($k \in [K]$) to the server. Afterwards, the server updates the communicated model with average aggregation as follows:

$$\psi_k^{t+1, 1} = \frac{1}{|\mathcal{S}_t|} \sum_{k \in \mathcal{S}_t} \psi_k^{t, \tau_c+1}. \quad (14)$$

After the model aggregation in Eq. (14), the communicated models at $(t+1)$ -th round are the same across all clients. In contrast, the personalized model is customized based on the specific data distribution of each client. As shown in Fig. 5, each client can choose arbitrary preference vectors, and the hypernetwork then provides the corresponding personalized models to the client. Then, each client can combine the personalized model with the communicated model, and the combined model can produce the desired results considering the client's preference over model performance and model fairness.

5 ALGORITHMIC ANALYSIS

In this section, we analyze performance guarantee of the trained model and the convergence rate of PraFFL. The proofs of this section are provided in the Appendix.

5.1 Learning Capabilities

Based on the properties of the weighted Tchebycheff function [26], we determine the following three main results:

- Existence of the Pareto optimal model;
- Condition of Pa model being Pareto optimal;
- The ability to find the Pareto front.

We analyze the model of an arbitrary client k . Given a preference vector λ in problem (10a), i -th objective can be expressed as $\mathcal{L}_i(x, y, \theta_k(\lambda))$, $\forall i \in \{1, 2\}$ over dataset \mathcal{D}_k . First, we analyze the existence of the Pareto optimal model.

THEOREM 5.1 (EXISTENCE). *Given a preference vector $\lambda \in \mathbb{R}_{\geq 0}^2$, problem (10) has at least one Pareto optimal solution.*

Theorem 5.1 shows that PraFFL has Pareto optimal solutions for any client's preference λ . After we determine the existence of Pareto optimality of the model, we then analyze the condition when a model is Pareto optimal. We have the following theorem:

THEOREM 5.2 (PARETO OPTIMALITY). *Given a preference vector $\lambda \in \mathbb{R}_{\geq 0}^2$, a model is weakly Pareto optimal if it minimizes problem (10). The model is Pareto optimal if and only if the optimal solution of problem (10) is unique.*

This theorem shows that PraFFL can achieve the Pareto optimal solution for the preference vector λ if the conditions in Theorem 5.2 are satisfied. Finally, we analyze the ability of PraFFL to find the Pareto front, and we have the following theorem:

THEOREM 5.3 (PARETO FRONT). *Let $\theta'_k \in \Theta$ be an optimal model for a given client's preference. Then, there exists a preference vector $\lambda \in \mathbb{R}_{\geq 0}^2$ such that we can obtain $\theta_k^*(\lambda) = \theta'_k$ from problem (10).*

Theorem 5.3 shows that the models can obtain the entire Pareto front. This is because, for any Pareto optimal model θ'_k , there is a preference vector λ that the model $\theta_k^*(\lambda)$ is Pareto optimal.

5.2 Convergence Analysis

In this subsection, we discuss the convergence properties of PraFFL. The optimization between the communicated model and the personalized model are correlated. We first prove that the communicated model converges linearly under the personalized FL framework. We then prove that the convergence rate of the personalized model is the same as that of the communicated model. Finally, we conclude that PraFFL also converges linearly.

The convergence analysis of problem (10) is difficult because the weighted Tchebycheff function is non-differentiable. To overcome this issue, we introduce a *smooth Tchebycheff function* as follows:

$$\min_{\theta_k} \tilde{g}(x, y, \theta_k(\lambda) | \lambda) = \min_{\theta_k} \frac{1}{\gamma} \log \sum_{i \in [2]} e^{\frac{\gamma \mathcal{L}_i(x, y, \theta_k(\lambda))}{\lambda_i}}, \quad (15)$$

where $\gamma > 0$ represents the smooth factor.

Before presenting convergence results, we list the following two commonly used assumptions.

ASSUMPTION 5.1. *The expectation of stochastic gradients is always bounded, i.e., for all $\phi_k^t \in \Phi$ and $\psi^t \in \Psi$, we have $\mathbb{E}[\|\nabla \tilde{g}\|^2] \leq G^2$.*

ASSUMPTION 5.2. *$\mathcal{L}_i(x, y, \theta_k(\lambda))$ is μ_i -strongly convex and L_i -smooth for all $k \in [K]$, $\lambda \in \Lambda$, and $\theta_k(\lambda) \in \Theta$.*

Based on the above assumptions, we can deduce the strong convex coefficient and smoothness coefficient of the smooth Tchebycheff function.

LEMMA 5.4 (CONVEXITY OF SMOOTH TCHEBYCHEFF FUNCTION). *If Assumption 5.2 is satisfied for $i \in [1, 2]$, then $\tilde{g}(x, y, \theta_k(\lambda))$ is $2 \log(\sum_{i \in [2]} e^{\frac{\mu_i}{2\lambda_i}})$ -strongly convex function, for $k \in [K]$ and $\lambda \in \Lambda$,*

LEMMA 5.5 (SMOOTHNESS OF SMOOTH TCHEBYCHEFF FUNCTION). *If Assumption 5.2 is satisfied for $i \in [1, 2]$, then $\tilde{g}(x, y, \theta_k(\lambda))$ is $\sum_{i \in [2]} \frac{L_i}{\lambda_i}$ -smooth, for $k \in [K]$.*

LEMMA 5.6 (CONVERGENCE OF THE COMMUNICATED MODEL [6]). *If the communicated model ψ is optimized by Fedavg [24] and given a constant $\zeta > 0$, then ψ converges to optimal communicated model ψ^* at a linear rate*

$$z(t) = \mathbb{E}[\|\psi^t - \psi^*\|^2] \leq (1 - \eta\zeta)^{t/2} \mathbb{E}[\|\psi^1 - \psi^*\|], \quad (16)$$

with a probability no smaller than $1 - te^{-100 \min(|X|^2 \log(|S_t|), d)}$.

Lemma 5.6 implies that in order to achieve a bound of $(1 - \eta\zeta)^{t/2} \mathbb{E}[\|\psi^1 - \psi^*\|] \leq \varepsilon$, we must run $O(\log(\frac{1}{\varepsilon}))$ iterations of gradient descent. This convergence rate is often called *linear convergence*.

For simplicity, let us denote $\check{\mu} = 2 \log(\sum_{i \in [2]} e^{\frac{\mu_i}{2\lambda_i}})$ and $\check{L} = \sum_{i \in [2]} \frac{L_i}{\lambda_i}$. The convergence speed of the personalized model is given by the following proposition.

PROPOSITION 5.7 (PROGRESS OF ONE STEP). *Under Assumptions 5.1 and 5.2, let client k get selected with probability p_k at each communication round t with decaying $\eta_t = \frac{2\check{\mu}}{(t+1)p_k}$, we have*

$$\begin{aligned} & \mathbb{E}[\|\phi_k^{t+1} - \phi_k^*\|^2] \\ & \leq (1 - \frac{2}{t+1}) \mathbb{E}[\|\phi_k^t - \phi_k^*\|^2] + \frac{8\check{\mu}^2 G \check{L}}{(t+1)^2 p_k^2} \sqrt{\mathbb{E}[\|\psi^t - \psi^*\|^2]} \\ & \quad + \frac{4\check{\mu}^2 G^2}{(t+1)^2 p_k^2} + (\frac{4\check{\mu}^2 \check{L}^2}{(t+1)^2 p_k^2} + \frac{2\check{\mu}}{t+1} (\check{L} - \check{\mu})) \mathbb{E}[\|\psi^t - \psi^*\|^2] \\ & \quad + \frac{4\check{\mu} \check{L}}{t+1} \sqrt{\mathbb{E}[\|\phi_k^t - \phi_k^*\|^2] \mathbb{E}[\|\psi^t - \psi^*\|^2]}. \end{aligned} \quad (17)$$

Proposition 5.7 shows the convergence speed of the personalized model is affected by the convergence speed of the communicated model, which is intuitively reasonable because these two types of models are optimized sequentially in our system. We further prove that each client's model $\theta_k(\lambda)$ also is linear convergence.

THEOREM 5.8 (CONVERGENCE OF PRAFFL). *If there exists a constant A such that $\frac{z(t+1)}{z(t)} \geq 1 - \frac{z(t)}{A}$, for $\lambda \in \Lambda$, then we have*

$$\mathbb{E}[\|\theta_k^t(\lambda) - \theta_k^*(\lambda)\|^2] = O(\log(\frac{1}{t})). \quad (18)$$

with a probability no smaller than $1 - te^{-100 \min(|X|^2 \log(|S_t|), d)}$.

Theorem 5.8 shows that PraFFL linearly converges to Pareto optimal solution $\theta_k^*(\lambda)$.

Table 2: Summary results of five different algorithms on four datasets. The average HV value is reported, as well as the average training time of all algorithms on each dataset.

Method	HV \uparrow			
	Synthetic	Compas	Bank	Adult
LFT+Ensemble	0.479	0.555	0.881	0.764
LFT+Fedavg	0.698	0.539	0.883	0.768
Agnosticfair	0.530	0.546	0.882	0.783
FairFed	0.342	0.507	0.878	0.269
FedFB	0.599	0.517	0.883	0.764
PraFFL	0.763	0.629	0.889	0.828

Method	Training Time (hours) \downarrow			
	Synthetic	Compas	Bank	Adult
LFT+Ensemble	0.048	1.943	5.430	8.006
LFT+Fedavg	0.059	1.047	3.228	15.097
Agnosticfair	0.018	1.147	3.909	9.246
FairFed	0.052	0.979	3.496	13.893
FedFB	0.020	1.024	3.197	8.016
PraFFL	0.164	1.357	5.155	11.544

6 NUMERICAL Experiments

In this section, we empirically compare our proposed PraFFL algorithm with five advanced baselines (LFT+Fedavg [20], LFT+Ensemble [40], Agnosticfair [8], FairFed [10], and FedFB [40]).

6.1 Experimental Settings

We report results from three runs on each dataset. PraFFL shows the solutions obtained by 1000 preference vectors in the experiment (in fact, any number of solutions can be obtained through PraFFL inference if a corresponding number of preference vectors are given). The total local epochs are set to 30 (i.e., $\tau_p + \tau_c = 30$). The batch size of preference vectors n_λ is set to 64. See Appendix A.1.1 for other detailed parameter settings. We use hypervolume (HV) [12] to measure the quality of the solution set obtained by each algorithm. The higher the quality of the solutions in satisfying the client’s preferences, the larger the HV value. Four widely used datasets are employed to conduct experiments, including SYNTHETIC [40], COMPAS [2], BANK [28] and ADULT [9].

6.2 Main Results

The results presented in Table 2 demonstrate that PraFFL is consistently superior to the performance of five baselines regarding HV. Our proposed PraFFL has the best HV value in the four datasets, which are 0.763, 0.629, 0.889, and 0.828, respectively. This is because our proposed method can infer any number of personalized models, thereby obtaining more solutions with different trade-offs between model performance and fairness. Additionally, Table 2 also shows the average training time of each algorithm. Although PraFFL runs slower than some baselines, its advantage is that once being trained, it can provide solutions for client’s arbitrary preferences in real time. Recall that other baselines require retraining the model if each client has more than one preference, and the training time increases linearly with the number of preferences (see Table 1).

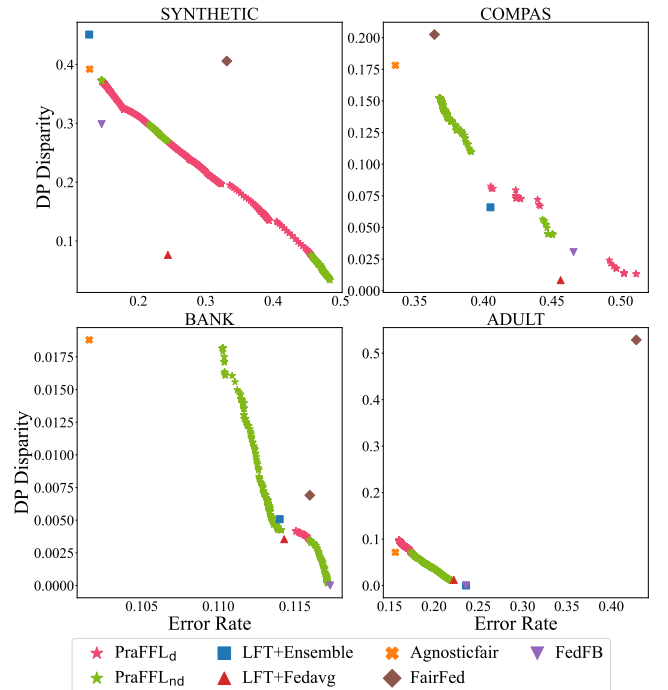


Figure 6: Comparison of solutions obtained by five algorithms on four datasets. We divide the solution set obtained by the PraFFL method into two categories: PraFFL_d and PraFFL_{nd} . PraFFL_d means that the solution is dominated (i.e., there is another algorithm that is better than the solutions in PraFFL_d), and PraFFL_{nd} means that the solution is non-dominated (i.e., there is no other solution that is better than the solutions in PraFFL_{nd}).

Moreover, Fig. 6 shows the final solutions obtained by the baselines and the non-dominated solutions obtained by PraFFL among 1000 solutions. According to the dominance relationship in Definition 3.1, we divide the solutions obtained by PraFFL into two categories (PraFFL_d and PraFFL_{nd}). PraFFL_d (red stars) are inferior to some baselines in some preferences. The solution set in PraFFL_{nd} (green stars) is superior to other baselines (it is the best trade-off between fairness and error rate for some specific preferences). Since the solution set of PraFFL covers the optimal trade-offs for most of the client’s preferences, the solution set obtained by PraFFL is better than the solution obtained by other algorithms. The advantage of PraFFL is that it can provide arbitrary solutions for clients with only one training. In addition, the Pareto front obtained by PraFFL on the COMPAS and BANK datasets can be further improved. There are two aspects that can further improve the learned Pareto front: (I) The data distribution of the training and testing set are not exactly the same. Obtaining a superior solution set on the training set may not necessarily lead to a superior solution set on the testing set; (II) Our optimization goals of model performance and fairness are not directly equivalent to optimizing the error rate and DP disparity (we conduct an experimental analysis of this aspect in the Appendix A.3.3). Therefore, these two aspects lead to a gap between the solution set we obtained and the optimal solution set, which motivates future research directions.

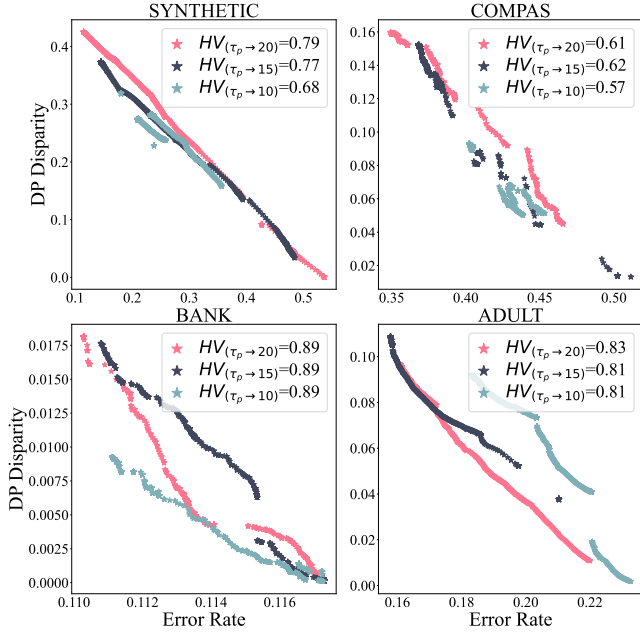


Figure 7: Solutions obtained by PraFFL under different τ_p .

6.3 Ablation Studies

This subsection investigates the impact of τ_p and the mapping of preferences to models. Due to space constraints, we further empirically show that our proposed algorithm is more beneficial under higher data heterogeneity. See the Appendix A.3.2 for details.

6.3.1 The effect of τ_p . We study the impact of different τ_p values in PraFFL. The distance between the solution set and the origin is called the convergence result of the solution set, and the smaller the distance is, the better the convergence result should be. As shown in Fig. 7, adjusting the value of τ_p is a trade-off problem. We can find that smaller τ_p generally has stronger convergence (i.e., closer to the origin), while larger τ_p tends to have a wider distribution of solution sets (i.e., the distinction for each preference is larger). This is because a smaller τ_p means that the client’s communicated model is trained for more times (i.e., $30 - \tau_p$), which is helpful to enhance the overall model performance, but the personalized model may be underfitting for some preferences. Instead, a larger τ_p will allow the personalized model to fully learn the user’s preferences while ignoring the performance of the communicated model. For instance, when $\tau_p = 10$ in COMPAS, the convergence results of the model are superior, but the underfitting of the preference vector results in the two objectives value clustering together for different user preferences. For the ADULT dataset, this may be due to its high data heterogeneity on different clients, which requires a higher τ_p (i.e., a larger τ_p is required to make the model optimal).

6.3.2 Different preferences of clients. We analyze the mapping from different preference vectors to their corresponding solution set on four datasets. For the simplicity of verifying the effectiveness of PraFFL, we assume that the preferences of all users are unchanged during inference. In Fig. 8, we can find that the solutions corresponding to different preferences are clearly distinguishable. This

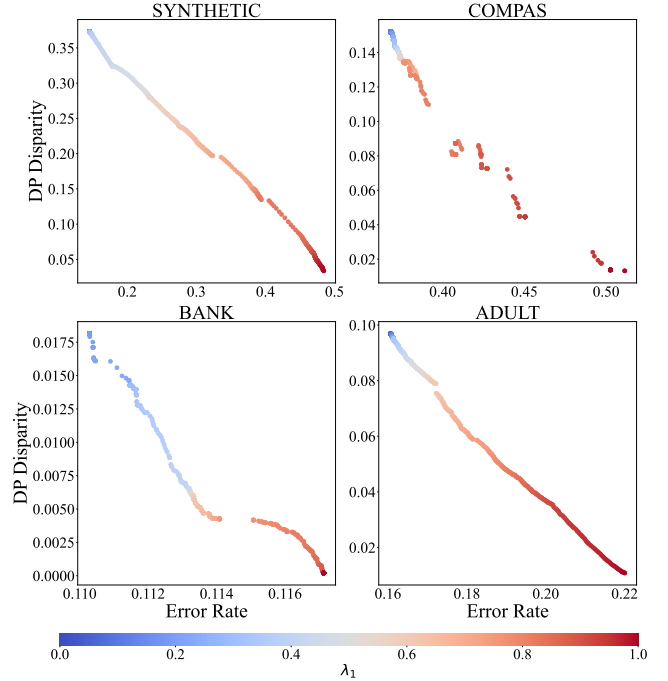


Figure 8: Mapping relationship from different preferences to model performance and fairness.

shows that PraFFL can assign a unique solution to each user’s different preferences. In addition, we observe that the Pareto front obtained by PraFFL on SYNTHETIC, BANK, and ADULT have a wide range, which indicates that PraFFL provide models for various preferences of clients. The learned Pareto front under COMPAS is slightly worse than that under the other three datasets, which may be due to data quality. In general, PraFFL can meet most of the preference requirements of clients based on the preference vectors they provide.

7 Conclusion and Future Works

Conclusion. In this work, we proposed a preference-aware scheme in fair federated learning (PraFFL), which is capable of providing models with different trade-offs to every client in real time. In the training phase, our proposed PraFFL does not require the assumption that the Pareto front is convex and preserves the client’s preference privacy. In the inference phase, the model obtained by PraFFL can be adaptively adjusted according to the client’s preferences. We theoretically prove that given a client’s preference, PraFFL can linearly converge to the Pareto optimal model and learn the entire Pareto front. Experimental results show that the solution set obtained by PraFFL on four datasets is well-performing, and the solutions obtained by PraFFL are the optimal choices for most of the client’s preferences compared to five advanced algorithms.

Future Works. Although our proposed PraFFL can achieve promising results on the four datasets, it still has room for improvement. The first direction is to improve the generalization ability of the learned Pareto front. The distribution of the training and testing dataset is inconsistent. A good solution set on the training dataset may not necessarily lead to a superior solution set on the

testing dataset. Therefore, the generalization of the learned Pareto front can be improved by regularization or using advanced data sampling strategies. In the second direction, the cross-entropy and fair loss function used in our work are not completely equivalent to the error rate and DP disparity formulations, respectively. To further improve the performance of PraFFL, a possible approach is to approximate the error rate and DP disparity formulations.

References

- [1] Annie Abay, Yi Zhou, Nathalie Baracaldo, Shashank Rajamoni, Ebube Chuba, and Heiko Ludwig. 2020. Mitigating bias in federated learning. *arXiv preprint arXiv:2012.02447* (2020).
- [2] Matias Barenstein. 2019. Propublica’s compas data revisited. *arXiv preprint arXiv:1906.04711* (2019).
- [3] Stephen P Boyd and Lieven Vandenbergh. 2004. *Convex optimization*. Cambridge university press.
- [4] Lingyang Chu, Lanjun Wang, Yanjie Dong, Jian Pei, Zirui Zhou, and Yong Zhang. 2021. Fedfair: Training fair models in cross-silo federated learning. *arXiv preprint arXiv:2109.05662* (2021).
- [5] Carlos A Coello Coello. 2007. *Evolutionary algorithms for solving multi-objective problems*. Springer.
- [6] Liam Collins, Hamed Hassani, Aryan Mokhtari, and Sanjay Shakkottai. 2021. Exploiting shared representations for personalized federated learning. In *International conference on machine learning*. PMLR, 2089–2099.
- [7] Yuyang Deng, Mohammad Mahdi Kamani, and Mehrdad Mahdavi. 2020. Distributionally robust federated averaging. *Advances in neural information processing systems* 33 (2020), 15111–15122.
- [8] Wei Du, Depeng Xu, Xintao Wu, and Hanghang Tong. 2021. Fairness-aware agnostic federated learning. In *Proceedings of the 2021 SIAM International Conference on Data Mining (SDM)*. SIAM, 181–189.
- [9] Dheeru Dua, Casey Graff, et al. 2017. UCI machine learning repository, 2017. URL <http://archive.ics.uci.edu/ml> 7, 1 (2017), 62.
- [10] Yahya H Ezzeldin, Shen Yan, Chaoyang He, Emilio Ferrara, and A Salman Avestimehr. 2023. Fairfed: Enabling group fairness in federated learning. In *Proceedings of the AAAI Conference on Artificial Intelligence*, Vol. 37. 7494–7502.
- [11] Michael Feldman, Sorella A Friedler, John Moeller, Carlos Scheidegger, and Suresh Venkatasubramanian. 2015. Certifying and removing disparate impact. In *proceedings of the 21th ACM SIGKDD international conference on knowledge discovery and data mining*. 259–268.
- [12] Carlos M Fonseca, Luis Paquete, and Manuel López-Ibáñez. 2006. An improved dimension-sweep algorithm for the hypervolume indicator. In *2006 IEEE international conference on evolutionary computation*. IEEE, 1157–1163.
- [13] Borja Rodríguez Gálvez, Filip Granqvist, Rogier van Dalen, and Matt Seigel. 2021. Enforcing fairness in private federated learning via the modified method of differential multipliers. In *NeurIPS 2021 Workshop Privacy in Machine Learning*.
- [14] Xiuting Gu, Zhu Tianqing, Jie Li, Tao Zhang, Wei Ren, and Kim-Kwang Raymond Choo. 2022. Privacy, accuracy, and model fairness trade-offs in federated learning. *Computers & Security* 122 (2022), 102907.
- [15] Shengyuan Hu, Zhiwei Steven Wu, and Virginia Smith. 2022. Fair federated learning via bounded group loss. *arXiv preprint arXiv:2203.10190* (2022).
- [16] Erin T Jacques, Corey H Basch, Joseph Fera, and Vincent Jones II. 2023. # StopAsianHate: A content analysis of TikTok videos focused on racial discrimination against Asians and Asian Americans during the COVID-19 pandemic. *Dialogues in Health* 2 (2023), 100089.
- [17] Xiao Jin, Pin-Yu Chen, Chia-Yi Hsu, Chia-Mu Yu, and Tianyi Chen. 2021. Cafe: Catastrophic data leakage in vertical federated learning. *Advances in Neural Information Processing Systems* 34 (2021), 994–1006.
- [18] Toshihiro Kamishima, Shotaro Akaho, Hideki Asoh, and Jun Sakuma. 2012. Fairness-aware classifier with prejudice remover regularizer. In *Machine Learning and Knowledge Discovery in Databases: European Conference, ECML PKDD 2012, Bristol, UK, September 24–28, 2012. Proceedings, Part II* 23. Springer, 35–50.
- [19] Jakub Konečný, H Brendan McMahan, Daniel Ramage, and Peter Richtárik. 2016. Federated optimization: Distributed machine learning for on-device intelligence. *arXiv preprint arXiv:1610.02527* (2016).
- [20] Jakub Konečný, H Brendan McMahan, Felix X Yu, Peter Richtárik, Ananda Theertha Suresh, and Dave Bacon. 2016. Federated learning: Strategies for improving communication efficiency. *arXiv preprint arXiv:1610.05492* 8 (2016).
- [21] Tian Li, Shengyuan Hu, Ahmad Beirami, and Virginia Smith. 2021. Ditto: Fair and robust federated learning through personalization. In *International conference on machine learning*. PMLR, 6357–6368.
- [22] Tian Li, Maziar Sanjabi, Ahmad Beirami, and Virginia Smith. 2019. Fair resource allocation in federated learning. *arXiv preprint arXiv:1905.10497* (2019).
- [23] Lingjuan Lyu, Xinyi Xu, Qian Wang, and Han Yu. 2020. Collaborative fairness in federated learning. *Federated Learning: Privacy and Incentive* (2020), 189–204.
- [24] Brendan McMahan, Eider Moore, Daniel Ramage, Seth Hampson, and Blaise Agüera y Arcas. 2017. Communication-efficient learning of deep networks from decentralized data. In *Artificial intelligence and statistics*. PMLR, 1273–1282.
- [25] Ninareh Mehrabi, Cyprien de Lichy, John McKay, Cynthia He, and William Campbell. 2022. Towards Multi-Objective Statistically Fair Federated Learning. (2022).
- [26] Kaisa Miettinen. 1999. *Nonlinear multiobjective optimization*. Vol. 12. Springer Science & Business Media.
- [27] Mehryar Mohri, Gary Sivek, and Ananda Theertha Suresh. 2019. Agnostic federated learning. In *International Conference on Machine Learning*. PMLR, 4615–4625.
- [28] Sérgio Moro, Paulo Cortez, and Paulo Rita. 2014. A data-driven approach to predict the success of bank telemarketing. *Decision Support Systems* 62 (2014), 22–31.
- [29] Zibin Pan, Shuyi Wang, Chi Li, Haijin Wang, Xiaoying Tang, and Junhua Zhao. 2023. Fedmdfg: Federated learning with multi-gradient descent and fair guidance. In *Proceedings of the AAAI Conference on Artificial Intelligence*, Vol. 37. 9364–9371.
- [30] Afroditi Papadaki, Natalia Martinez, Martin Bertran, Guillermo Sapiro, and Miguel Rodrigues. 2022. Minimax demographic group fairness in federated learning. In *Proceedings of the 2022 ACM Conference on Fairness, Accountability, and Transparency*. 142–159.
- [31] Afroditi Papadaki, Natalia Martinez, Martin Bertran, Guillermo Sapiro, and Miguel Rodrigues. 2024. Federated Fairness without Access to Sensitive Groups. *arXiv preprint arXiv:2402.14929* (2024).
- [32] Yuji Roh, Kangwook Lee, Steven Euijong Whang, and Changho Suh. 2020. Fairbatch: Batch selection for model fairness. *arXiv preprint arXiv:2012.01696* (2020).
- [33] Teresa Salazar, Miguel Fernandes, Helder Araújo, and Pedro Henriques Abreu. 2023. Fair-fate: Fair federated learning with momentum. In *International Conference on Computational Science*. Springer, 524–538.
- [34] Karan Singhal, Hakim Sidahmed, Zachary Garrett, Shanshan Wu, John Rush, and Sushant Prakash. 2021. Federated reconstruction: Partially local federated learning. *Advances in Neural Information Processing Systems* 34 (2021), 11220–11232.
- [35] Alysa Ziyang Tan, Han Yu, Lizhen Cui, and Qiang Yang. 2022. Towards personalized federated learning. *IEEE Transactions on Neural Networks and Learning Systems* (2022).
- [36] Zheng Wang, Xiaoliang Fan, Jianzhong Qi, Chenglu Wen, Cheng Wang, and Rongshan Yu. 2021. Federated learning with fair averaging. *arXiv preprint arXiv:2104.14937* (2021).
- [37] Han Yu, Zelei Liu, Yang Liu, Tianjian Chen, Mingshu Cong, Xi Weng, Dusit Niyato, and Qiang Yang. 2020. A fairness-aware incentive scheme for federated learning. In *Proceedings of the AAAI/ACM Conference on AI, Ethics, and Society*. 393–399.
- [38] Honglin Yuan, Warren Richard Morningstar, Lin Ning, and Karan Singhal. 2021. What Do We Mean by Generalization in Federated Learning?. In *International Conference on Learning Representations*.
- [39] Xubo Yue, Maher Nouiheed, and Raed Al Kontar. 2023. Gifair-fl: A framework for group and individual fairness in federated learning. *INFORMS Journal on Data Science* 2, 1 (2023), 10–23.
- [40] Yuchen Zeng, Hongxu Chen, and Kangwook Lee. 2021. Improving fairness via federated learning. *arXiv preprint arXiv:2110.15545* (2021).
- [41] Brian Hu Zhang, Blake Lemoine, and Margaret Mitchell. 2018. Mitigating unwanted biases with adversarial learning. In *Proceedings of the 2018 AAAI/ACM Conference on AI, Ethics, and Society*. 335–340.
- [42] Daniel Yue Zhang, Ziyi Kou, and Dong Wang. 2020. Fairfl: A fair federated learning approach to reducing demographic bias in privacy-sensitive classification models. In *2020 IEEE International Conference on Big Data (Big Data)*. IEEE, 1051–1060.

A Appendix

A.1 Experimental Details

A.1.1 Experimental Parameters. The total communication rounds T is set to 10, and the batch size of data is 128 in the neural network training. We use Adam as optimizer and the learning rate η is 0.005. The smooth factor of smooth Tchebycheff function is set to one. The reference point \mathbf{r} in calculating hypervolume is set to (1, 1).

A.1.2 Dataset. According to the setting of [10, 40], the COMPAS and ADULT datasets have two clients, while the SYNTHETIC and BANK have three clients. This setting is common in cross-silo FL.

In Section A.3.1, we will conduct experiments on more clients. The information of the four datasets is as follows:

- **SYNTHETIC [40]**: Synthetic is an artificially generated dataset containing 5000 samples with two non-sensitive features and a binary sensitive feature.
- **COMPAS [2]**: Compas contains 7214 samples, 8 non-sensitive features, and 2 sensitive features (i.e., gender and race).
- **BANK [28]**: Bank contains 45211 samples, 13 non-sensitive features, and one sensitive feature (i.e., age).
- **ADULT [9]**: Adult contains 48842 samples, with 13 non-sensitive features and one sensitive feature (i.e., gender).

In the three real-world datasets, we split 30% of the data into the test set, and the other 70% of the data are split into the training set and validation set with a ratio of 9:1. Furthermore, we select the model that performs best in the validation set for testing.

A.1.3 Neural Network Architecture. The architecture of the communicated model ψ is as follow:

$$\begin{aligned} \psi(\mathbf{x}) : \mathbf{x} &\rightarrow \text{Linear}(|\mathbf{x}|, 4) \rightarrow \text{ReLU} \\ &\rightarrow \text{Linear}(4, 4) \rightarrow \text{ReLU} \rightarrow \mathbf{x}_{\text{mid}}, \end{aligned} \quad (19)$$

where \mathbf{x} represent features of dataset. The architecture of personalized model ϕ is as follow:

$$\begin{aligned} \phi(\mathbf{x}_{\text{mid}}) : \mathbf{x}_{\text{mid}} &\rightarrow \text{Linear}(4, 16) \rightarrow \text{ReLU} \\ &\rightarrow \text{Linear}(4, 4) \rightarrow \text{ReLU} \\ &\rightarrow \text{Linear}(4, 8) \rightarrow \text{ReLU} \\ &\rightarrow \text{Linear}(4, 1) \rightarrow \text{Sigmoid}. \end{aligned} \quad (20)$$

The architecture of hypernetwork $\beta(\lambda)$ is as follow:

$$\beta(\lambda) : \lambda \rightarrow \text{Linear}(|\lambda|, |\phi|), \quad (21)$$

where λ is preference vector, and the hypernetwork maps the preference vector to the personalized model ϕ .

A.2 Proofs

A.2.1 Proof of Theorem 5.1.

PROOF. Suppose that none of the optimal solution (i.e., ϕ_k) in problem (10) is Pareto optimal. Let $\theta_k^*(\lambda) \in \Phi$ be an optimal solution to problem (10). Since we assume that it is not Pareto optimal, there must exist a model $\theta'_k(\lambda) \in \Phi$ which is not optimal for problem (10) but for which $\mathcal{L}_i(\mathbf{x}, y, \theta'_k(\lambda)) \leq \mathcal{L}_i(\mathbf{x}, y, \theta_k^*(\lambda)), \forall i \in \{1, 2\}$ and $\mathcal{L}_i(\mathbf{x}, y, \theta'_k(\lambda)) < \mathcal{L}_i(\mathbf{x}, y, \theta_k^*(\lambda)), \exists i \in \{1, 2\}$. Therefore, we have

$$\mathcal{L}_i(\mathbf{x}, y, \theta'_k(\lambda)) \leq \mathcal{L}_i(\mathbf{x}, y, \theta_k^*(\lambda)), \forall i \in \{1, 2\}. \quad (22)$$

We substitute this inequality into the smooth Tchebycheff function and get the following inequality

$$\frac{1}{\gamma} \log \sum_{i \in [2]} e^{\frac{\mathcal{L}_i(\mathbf{x}, y, \theta'_k(\lambda))}{\lambda_i}} < \frac{1}{\gamma} \log \sum_{i \in [2]} e^{\frac{\mathcal{L}_i(\mathbf{x}, y, \theta_k^*(\lambda))}{\lambda_i}}. \quad (23)$$

This means θ'_k is optimal of problem (10), but we suppose θ_k^* is optimal of problem (10). This contradiction completes the proof. \square

Algorithm 1: PraFFL

Input : $K, \mathcal{D}_{k \in [K]}, T, \tau_c, \tau_p, \eta, n_\lambda, p, \check{\lambda}$
Output : $\{\psi_k^{T,1}\}_{k \in [K]}$ and $\{\beta_k^{T,1}\}_{k \in [K]}$

- 1 Each client initializes a hypernetwork $\beta_k^{1,1}$;
- 2 **for** $t = 1, \dots, (T - 1)$ **do**
- 3 Server randomly selects a subset S_t with $\lceil pK \rceil$ clients from K clients and sends aggregated model $\psi_k^{t,1}$ to them;
- 4 **for** client $k \in S_t$ in parallel **do**
- 5 // Optimize the communicated model
- 6 **for** $s = 1, \dots, \tau_c$ **do**
- 7 Update $\psi_k^{t,s+1}$ by Eq. (11);
- 8 // Optimize the hypernetwork
- 9 **for** $j = 1, \dots, \tau_p$ **do**
- 10 Sample preference vectors $\{\lambda^{(i)}\}_{i \in [n_\lambda]} \subseteq \Lambda$;
- 11 Update $\beta_k^{t,j+1}$ by Eq. (13);
- 12 // Server aggregate the communicated model
- 13 $\psi_k^{t+1,1} = \frac{1}{|S_t|} \sum_{k \in S_t} \psi_k^{t,\tau_c+1}$
- 14 **return** $\{\psi_k^{T,1}\}_{k \in [K]}$ and $\{\beta_k^{T,1}\}_{k \in [K]}$

A.2.2 Proof of Theorem 5.2.

PROOF. We suppose that $\theta_k^*(\lambda)$ is not Pareto optimal. By the definition of Pareto optimality (Definition 3.2), there exists another model $\theta'_k(\lambda) \in \Theta$ such that $\mathcal{L}(\mathbf{x}, y, \theta'_k) < \mathcal{L}(\mathbf{x}, y, \theta_k^*)$. Therefore, we have the following inequality

$$\mathcal{L}_i(\mathbf{x}, y, \theta'_k(\lambda)) \leq \mathcal{L}_i(\mathbf{x}, y, \theta_k^*(\lambda)), \forall i \in \{1, 2\}. \quad (24)$$

We also can obtain inequality (23), which contradicts the assumption, so $\theta_k^*(\lambda)$ is Pareto optimal for problem (10). \square

A.2.3 Proof of Theorem 5.3.

PROOF. Given a preference vector $\lambda \triangleq (\lambda_i > 0, i \in \{1, 2\})$, let θ_k^* is defined as follows:

$$\theta_k^*(\lambda) \triangleq \arg \min_{\theta_k \in \Theta} \bar{g}(\mathbf{x}, y, \theta_k(\lambda) | \lambda). \quad (25)$$

We suppose that $\theta_k^*(\lambda)$ is not Pareto optimal. By the definition of Pareto optimality (Definition 2.2), there exists another personalized model $\theta'_k(\lambda) \in \Phi$ such that $\mathcal{L}(\mathbf{x}, y, \theta'_k(\lambda)) < \mathcal{L}(\mathbf{x}, y, \theta_k^*(\lambda))$. Therefore, we have the following inequality:

$$\mathcal{L}_i(\mathbf{x}, y, \theta'_k(\lambda)) \leq \mathcal{L}_i(\mathbf{x}, y, \theta_k^*(\lambda)), \forall i \in \{1, 2\}. \quad (26)$$

We also can obtain inequality (23), which contradicts the assumption, so θ_k^* is Pareto optimal for problem (10). \square

A.2.4 Proof of Lemma 5.4. First, we give the following definition of strong convexity, with which we prove Lemma 5.4.

DEFINITION A.1. Define a function \mathcal{F}_i is μ_i -strongly convex if it is continuously differentiable and there exists a constant $\mu_i > 0$ such that for any $\phi_k^{(a)}, \phi_k^{(b)} \in \Phi, \psi^{(a)}, \psi^{(b)} \in \Psi, \lambda \in \Lambda$, and $(x, y) \in \mathcal{D}_k$,

$$\begin{aligned} & \left(\left\| \nabla_{\phi_k} \mathcal{F}_i(x, y, \theta_k^{(a)}(\lambda)) - \nabla_{\phi_k} \mathcal{F}_i(x, y, \theta_k^{(b)}(\lambda)) \right\| \right. \\ & \left. \left\| \nabla_{\psi} \mathcal{F}_i(x, y, \theta_k^{(a)}(\lambda)) - \nabla_{\psi} \mathcal{F}_i(x, y, \theta_k^{(b)}(\lambda)) \right\| \right) \\ & \geq \mu_i \left(\left\| \phi_k^{(a)} - \phi_k^{(b)} \right\| \right). \end{aligned} \quad (27)$$

PROOF. Given loss function $\mathcal{L}_i(x, y, \theta(\lambda))$ is μ_i -strongly convex for $i = 1, 2$ and $\lambda \in \Lambda$, we now prove that the smooth Tchebycheff function $\tilde{g}(x, y, \theta(\lambda) \mid \lambda)$ is $2\log(\sum_{i \in [3]} e^{\frac{\mu_i}{2\lambda_i}})$ -strongly convex for both the personalized model ϕ_k and the communicated model ψ_k for $k = 1, \dots, K$. We take ϕ_k as an example, and let $\tilde{g}(\phi_k)$ and $\mathcal{L}_i(\phi_k)$ be simply the parameter ϕ_k optimized by \tilde{g} and \mathcal{L}_i , respectively. Let $z \in [0, 1]$, we start from the definition of strong convexity to obtain the strong convexity coefficient of \tilde{g} .

$$\tilde{g}_i(z\phi_k^{(a)} + (1-z)\phi_k^{(b)} \mid \lambda) \quad (28)$$

$$= \frac{1}{\gamma} \log \left(\sum_{i \in [3]} e^{\gamma(\mathcal{L}_i(z\phi_k^{(a)} + (1-z)\phi_k^{(b)})) / \lambda_i} \right) \quad (29)$$

$$\leq \frac{1}{\gamma} \log \left(\sum_{i \in [3]} e^{\gamma(z\mathcal{L}_i(\phi_k^{(a)}) + (1-z)\mathcal{L}_i(\phi_k^{(b)})) - \frac{\mu_i}{2} z(1-z) \|\phi_k^{(a)} - \phi_k^{(b)}\| / \lambda_i} \right) \quad (30)$$

$$\leq \frac{1}{\gamma} \log \left(\sum_{i \in [3]} e^{\gamma(z\mathcal{L}_i(\phi_k^{(a)}) + (1-z)\mathcal{L}_i(\phi_k^{(b)})) / \lambda_i} \right) \quad (31)$$

$$+ \frac{1}{\gamma} \log \left(\sum_{i \in [3]} e^{-\gamma \frac{\mu_i}{2\lambda_i} z(1-z) \|\phi_k^{(a)} - \phi_k^{(b)}\|} \right) \quad (32)$$

$$= \frac{1}{\gamma} \log \left(\sum_{i \in [3]} e^{\gamma(z\mathcal{L}_i(\phi_k^{(a)}) + (1-z)\mathcal{L}_i(\phi_k^{(b)})) / \lambda_i} \right) \quad (33)$$

$$- \log \left(\sum_{i \in [3]} e^{\frac{\mu_i}{2\lambda_i}} \right) \cdot z(1-z) \|\phi_k^{(a)} - \phi_k^{(b)}\| \quad (34)$$

$$= \frac{z}{\gamma} \log \left(\sum_{i \in [3]} e^{\gamma(\mathcal{L}_i(\phi_{k,a})) / \lambda_i} \right) + \frac{1-z}{\gamma} \log \left(\sum_{i \in [3]} e^{\gamma(\mathcal{L}_i(\phi_{k,b})) / \lambda_i} \right) \quad (35)$$

$$- \log \left(\sum_{i \in [3]} e^{\frac{\mu_i}{2\lambda_i}} \right) \cdot z(1-z) \|\phi_k^{(a)} - \phi_k^{(b)}\|. \quad (36)$$

□

A.2.5 Proof of Lemma 5.5. We give the following definition of smoothness.

DEFINITION A.2. Define a function $\mathcal{F}_i(x, y, \theta_k(\lambda))$ is L_i -smooth if it is continuously differentiable and there exists a constant $L_i > 0$ such that for any $\phi_k^{(a)}, \phi_k^{(b)} \in \Phi, \psi^{(a)}, \psi^{(b)} \in \Psi, (x, y) \in \mathcal{D}_k$, and

$\lambda \in \Lambda$,

$$\begin{aligned} & \left(\left\| \nabla_{\phi_k} \mathcal{F}_i(x, y, \theta_k^{(a)}(\lambda)) - \nabla_{\phi_k} \mathcal{F}_i(x, y, \theta_k^{(b)}(\lambda)) \right\| \right. \\ & \left. \left\| \nabla_{\psi} \mathcal{F}_i(x, y, \theta_k^{(a)}(\lambda)) - \nabla_{\psi} \mathcal{F}_i(x, y, \theta_k^{(b)}(\lambda)) \right\| \right) \\ & \leq L_i \left(\left\| \phi_k^{(a)} - \phi_k^{(b)} \right\| \right). \end{aligned} \quad (37)$$

PROOF. Given loss function $\mathcal{L}_i(x, y, \theta(\lambda))$ is L_i -smooth for $i = 1, 2$ and $\lambda \in \Lambda$, we now prove that the smooth Tchebycheff function $\tilde{g}(x, y, \theta(\lambda) \mid \lambda)$ is $\frac{L_i}{\lambda_i}$ -smooth for both the personalized model ϕ_k and the communicated model ψ_k for $k = 1, \dots, K$. We take ϕ_k as an example, and let $\tilde{g}(\phi_k)$ and $\mathcal{L}_i(\phi_k)$ be simply the parameter ϕ_k optimized by \tilde{g} and \mathcal{L}_i , respectively. We start from the definition of smoothness to obtain the smooth coefficient of \tilde{g} . Due to the chain rule $\nabla \tilde{g}(\phi_k) = \sum_{i \in [2]} \nabla \mathcal{L}_i(\phi_k) \nabla \mathcal{L}_i \tilde{g}(\phi_k)$, we can calculate $\nabla \mathcal{L}_i \tilde{g}(\phi_k) = \sum_{i \in [2]} \frac{e^{\mathcal{L}_i(\phi_k)}}{\lambda_i \sum_{i \in [2]} e^{\mathcal{L}_i(\phi_k)}}$. After that, we start from the following equation:

$$\begin{aligned} & \left\| \nabla \tilde{g}(\phi_k^{(a)}) - \nabla \tilde{g}(\phi_k^{(b)}) \right\| \\ & = \left\| \sum_{i \in [2]} \nabla \mathcal{L}_i(\phi_k^{(a)}) \nabla \mathcal{L}_i \tilde{g}(\phi_k^{(a)}) - \nabla \mathcal{L}_i(\phi_k^{(b)}) \nabla \mathcal{L}_i \tilde{g}(\phi_k^{(b)}) \right\| \end{aligned} \quad (38)$$

$$\begin{aligned} & = \left\| \sum_{i \in [2]} \frac{e^{\mathcal{L}_i(\phi_k^{(a)})}}{\lambda_i \sum_{i \in [2]} e^{\mathcal{L}_i(\phi_k^{(a)})}} \nabla \mathcal{L}_i(\phi_k^{(a)}) \right. \\ & \quad \left. - \sum_{i \in [2]} \frac{e^{\mathcal{L}_i(\phi_k^{(b)})}}{\lambda_i \sum_{i \in [2]} e^{\mathcal{L}_i(\phi_k^{(b)})}} \nabla \mathcal{L}_i(\phi_k^{(b)}) \right\| \end{aligned} \quad (39)$$

$$\leq \sum_{i \in [2]} \frac{1}{\lambda_i} \left\| \nabla \mathcal{L}_i(\phi_k^{(a)}) - \nabla \mathcal{L}_i(\phi_k^{(b)}) \right\| \quad (40)$$

$$\leq \sum_{i \in [2]} \frac{L_i}{\lambda_i} \left\| \phi_k^{(a)} - \phi_k^{(b)} \right\|^2. \quad (41)$$

The last step is due to the smoothness of \mathcal{L}_i . Then, we can also get the smoothness coefficient of $\tilde{g}(\phi)$,

$$\left\| \nabla \tilde{g}(\phi^{(a)}) - \nabla \tilde{g}(\phi^{(b)}) \right\| \leq \sum_{i \in [2]} \frac{L_i}{\lambda_i} \left\| \phi^{(a)} - \phi^{(b)} \right\|^2. \quad (42)$$

□

A.2.6 Proof of Proposition 5.7.

PROOF. We now prove an upper bound of the difference between the personalized model on any client (take client k as an example) ϕ_k and the optimal personalized model ϕ_k^* . Let I_k^t indicate if user k

is selected at the t -round, and $\mathbb{E} [I_k^t] = p_k$. We have

$$\begin{aligned} & \mathbb{E} [\|\phi_k^{t+1} - \phi_k^*\|^2] \\ &= \mathbb{E} [\|\phi_k^t - \eta I_k^t \nabla \bar{g}(\phi_k^t; \psi^t) - \phi_k^*\|^2] \end{aligned} \quad (43)$$

$$\begin{aligned} &= \mathbb{E} [\|\phi_k^t - \phi_k^*\|^2] + \eta^2 \mathbb{E} [\|I_k^t \bar{g}(\phi_k^t; \psi^t)\|^2] \\ &+ 2\eta \mathbb{E} [p_k \nabla \bar{g}(\phi_k^t; \psi^t)^T (\phi_k^* - \phi_k^t)] \end{aligned} \quad (44)$$

$$\begin{aligned} &\stackrel{(a)}{\leq} (1 - \eta p_k \check{\mu}) \mathbb{E} [\|\phi_k^t - \phi_k^*\|^2] + \underbrace{\eta^2 \mathbb{E} [\|\nabla \bar{g}(\phi_k^t; \psi^t)\|^2]}_{C_1} \\ &+ \underbrace{2\eta p_k \mathbb{E} [\bar{g}(\phi_k^*; \psi^t) - \bar{g}(\phi_k^t; \psi^t)]}_{C_2}, \end{aligned} \quad (45)$$

where (a) is due to the smoothness of \bar{g} . We then find the upper bounds of C_1 and C_2 , respectively. For C_1 ,

$$\begin{aligned} &\eta^2 \mathbb{E} [\|\nabla \bar{g}(\phi_k^t; \psi^t)\|^2] \\ &= \eta^2 \mathbb{E} [\|\bar{g}(\phi_k^t; \psi^t) - \nabla \bar{g}(\phi_k^t; \psi^t) + \nabla \bar{g}(\phi_k^t; \psi^t)\|^2] \\ &= 2\eta^2 \mathbb{E} [\|\nabla \bar{g}(\phi_k^t; \psi^t)\| \|\bar{g}(\phi_k^t; \psi^t) - \nabla \bar{g}(\phi_k^t; \psi^t)\|] \\ &+ \eta^2 \mathbb{E} [\|\nabla \bar{g}(\phi_k^t; \psi^t)\|^2] + \eta^2 \mathbb{E} [\|\nabla \bar{g}(\phi_k^t; \psi^t) - \nabla \bar{g}(\phi_k^t; \psi^t)\|^2] \end{aligned} \quad (46)$$

$$\begin{aligned} &\stackrel{(b)}{\leq} \eta^2 \mathbb{E} [\|\nabla \bar{g}(\phi_k^t; \psi^t)\|^2] + 2\eta^2 \check{L} \mathbb{E} [\|\nabla \bar{g}(\phi_k^t; \psi^t)\| \|\psi^t - \psi^t\|] \\ &+ \eta^2 \check{L}^2 \mathbb{E} [\|\psi^t - \psi^t\|^2], \end{aligned} \quad (48)$$

where (b) is due to the convexity of \bar{g} . Then, we continue to find the upper bound of C_2 ,

$$\begin{aligned} &2\eta p_k \mathbb{E} [\bar{g}(\phi_k^*; \psi^t) - \bar{g}(\phi_k^t; \psi^t)] \\ &\stackrel{(c)}{\leq} 2\eta p_k \mathbb{E} [\bar{g}(\phi_k^*; \psi^t) - \bar{g}(\phi_k^t; \psi^t) + \eta p_k (\check{L} - \check{\mu}) \|\psi^t - \psi^t\|^2] \\ &+ \mathbb{E} [(\nabla \bar{g}(\phi_k^*; \psi^t) - \nabla \bar{g}(\phi_k^t; \psi^t))^T (\psi^t - \psi^t)] \end{aligned} \quad (49)$$

$$\begin{aligned} &\stackrel{(d)}{\leq} 2\eta p_k \mathbb{E} [\bar{g}(\phi_k^*; \psi^t) - \bar{g}(\phi_k^t; \psi^t) + \eta p_k (\check{L} - \check{\mu}) \|\psi^t - \psi^t\|^2] \\ &+ 2\eta p_k \check{L} \mathbb{E} [\|\phi_k^t - \phi_k^*\| \|\psi^t - \psi^t\|], \end{aligned} \quad (50)$$

where (c) uses the smoothness and convexity of \bar{g} . (d) uses the convexity of \bar{g} . So far, we have found the upper bounds of C_1 and C_2 . We then plugging their upper bounds Eq. (48) and Eq. (50) into

Eq. (45), as follows:

$$\begin{aligned} &\mathbb{E} [\|\phi_k^{t+1} - \phi_k^*\|^2] \\ &\leq (1 - \eta p_k \check{\mu}) \mathbb{E} [\|\phi_k^t - \phi_k^*\|^2] + \eta^2 \mathbb{E} [\|\nabla \bar{g}(\phi_k^t; \psi^t)\|^2] \\ &+ 2\eta^2 \check{L} \mathbb{E} [\|\nabla \bar{g}(\phi_k^t; \psi^t)\| \|\psi^t - \psi^t\|] \\ &+ \eta^2 \check{L}^2 \mathbb{E} [\|\psi^t - \psi^t\|^2] + 2\eta p_k \mathbb{E} [\bar{g}(\phi_k^*; \psi^t) - \bar{g}(\phi_k^t; \psi^t)] \\ &+ 2\eta p_k \check{L} \mathbb{E} [\|\phi_k^t - \phi_k^*\| \|\psi^t - \psi^t\|] \\ &+ \eta p_k (\check{L} - \check{\mu}) \mathbb{E} [\|\psi^t - \psi^t\|^2] \end{aligned} \quad (51)$$

$$\begin{aligned} &\stackrel{(e)}{\leq} (1 - \eta p_k \check{\mu}) \mathbb{E} [\|\phi_k^t - \phi_k^*\|^2] + \eta^2 \mathbb{E} [\|\nabla \bar{g}(\phi_k^t; \psi^t)\|^2] \\ &+ 2\eta^2 \check{L} \sqrt{\mathbb{E} [\|\nabla \bar{g}(\phi_k^t; \psi^t)\|^2] \mathbb{E} [\|\psi^t - \psi^t\|^2]} \\ &+ \eta^2 \check{L}^2 \mathbb{E} [\|\psi^t - \psi^t\|^2] \\ &+ 2\eta p_k \check{L} \sqrt{\mathbb{E} [\|\phi_k^t - \phi_k^*\|^2] \mathbb{E} [\|\psi^t - \psi^t\|^2]} \\ &+ \eta p_k (\check{L} - \check{\mu}) \mathbb{E} [\|\psi^t - \psi^t\|^2] \end{aligned} \quad (52)$$

$$\begin{aligned} &\stackrel{(f)}{\leq} (1 - \eta p_k \check{\mu}) \mathbb{E} [\|\phi_k^t - \phi_k^*\|^2] + \eta^2 G^2 + 2\eta^2 G \check{L} \sqrt{\mathbb{E} [\|\psi^t - \psi^t\|^2]} \\ &+ (\eta^2 \check{L}^2 + \eta p_k (\check{L} - \check{\mu})) \mathbb{E} [\|\psi^t - \psi^t\|^2] \\ &+ 2\eta p_k \check{L} \sqrt{\mathbb{E} [\|\phi_k^t - \phi_k^*\|^2] \mathbb{E} [\|\psi^t - \psi^t\|^2]}, \end{aligned} \quad (53)$$

where (e) is due to the Cauchy-Schwarz inequality and $\mathbb{E} [\bar{g}(\phi_k^*; \psi^t) - \bar{g}(\phi_k^t; \psi^t)] \leq 0$. (f) holds because the norm of the squared gradient is bounded by G^2 (Assumption 5.1). \square

A.2.7 Proof of Theorem 5.8.

PROOF. There exists $C < \infty$ such that for any client $k \in [K]$, $C > \frac{\mathbb{E} [\|\phi_k^0 - \phi_k^*\|^2]}{g(0)}$, we have

$$\mathbb{E} [\|\phi_k^0 - \phi_k^*\|^2] \leq Cg(0). \quad (54)$$

If $\mathbb{E} [\|\phi_k^t - \phi_k^*\|^2] \leq Cz(t)$ holds, then for $t+1$,

$$\begin{aligned} &\mathbb{E} [\|\phi_k^{t+1} - \phi_k^*\|^2] \\ &\leq (1 - \frac{2z(t)}{A})Cz(t) + \frac{z(t)^2}{A} \frac{4\sqrt{C}}{\check{\mu}} + \frac{z(t)^2}{A} \frac{2(\check{L} - \check{\mu})}{\check{\mu}} \\ &+ \frac{z(t)^2}{A} \frac{4}{Ap_k^2 \check{\mu}^2} (G^2 + \check{L}^2 z(t) + 2G\check{L}\sqrt{z(t)}) \end{aligned} \quad (55)$$

$$\stackrel{(a)}{\leq} (1 - \frac{2z(t)}{A})Cz(t) + \frac{Cz(t)^2}{A} \quad (56)$$

$$= (1 - \frac{z(t)}{A})Cz(t) \quad (57)$$

$$\stackrel{(b)}{\leq} Cz(t+1) \quad (58)$$

$$\stackrel{(c)}{\leq} C \cdot O(\log(\frac{1}{t+1})), \quad (59)$$

where (a) holds because C is a sufficiently large number such that coefficient of $\frac{z(t)^2}{A}$ is smaller than C . (b) is due to the condition $\frac{z(t+1)}{z(t)} \geq 1 - \frac{z(t)}{A}$. (c) is due to the Lemma 5.6. \square

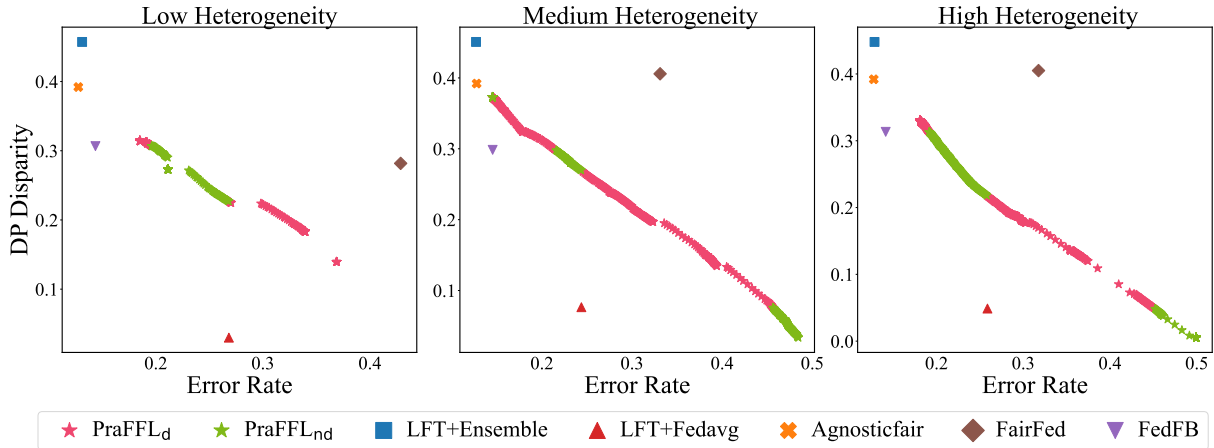


Figure 9: Accuracy-fairness solutions on the SYNTHETIC dataset with three clients having different heterogeneity distributions of the sensitive feature. The sensitive feature of SYNTHETIC has two groups. Each group of the sensitive feature is divided into three parts and assigned to three clients. Let A denote the proportion of the first group of sensitive features (e.g., male) assigned to the three clients. Let B denote the proportion of the second group of sensitive features (e.g., female) assigned to the three clients. (a) A : 33%, 33%, 34% and B : 33%, 33%, 34%. (b) A : 50%, 30%, 20% and B : 20%, 40%, 40%. (c) A : 70%, 10%, 20% and B : 10%, 80%, 10%.

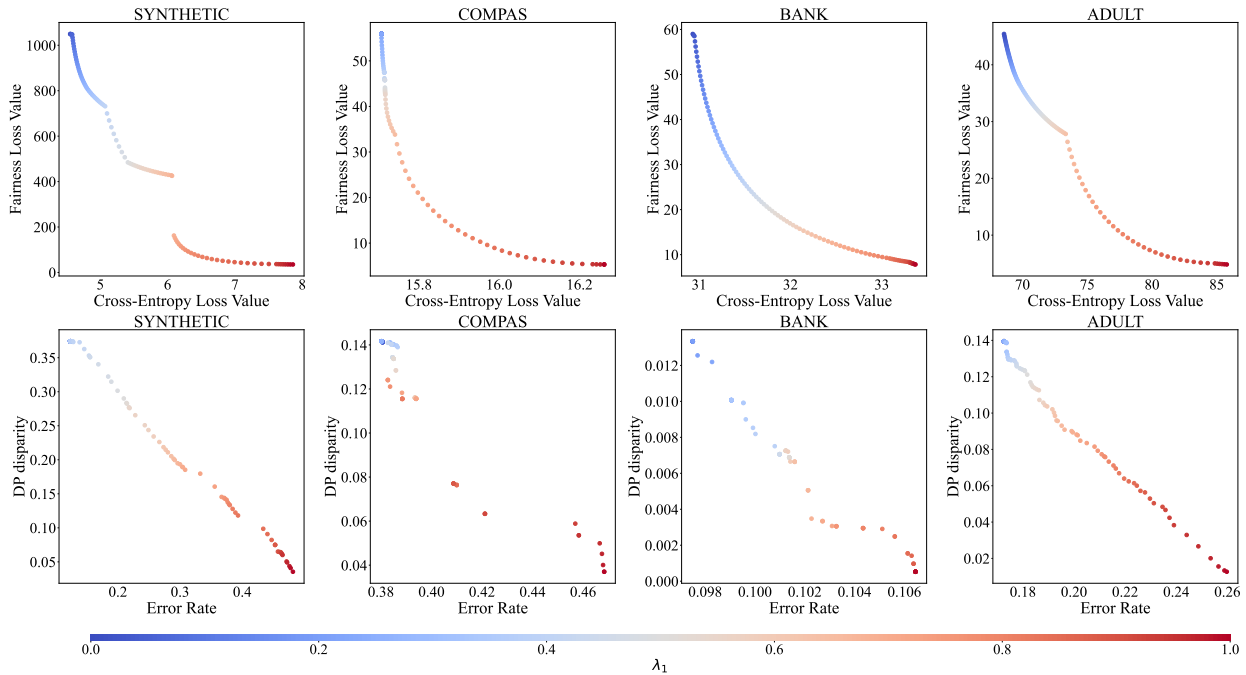


Figure 10: Comparison of the values of the two loss functions and the metrics values in the validation dataset under different preference vectors.

A.3 Additional Experiments

A.3.1 The effect of the number of clients. Table 3 shows the results under different numbers of clients on the SYNTHETIC dataset. Our proposed PraFFL achieves the best performance compared to the other five baselines in all settings in Table 3.

A.3.2 The effect of data heterogeneity. We examine the error rate and DP Disparity obtained by each algorithm under different heterogeneous levels on the sensitive features. As in [40], we study

three heterogeneous scenarios. Fig. 9 shows the performance of the algorithms under three different heterogeneity levels. We can observe that our proposed PraFFL are robust than the other five baselines under different heterogeneous levels. Compared with the other five algorithms, the number of solutions of PraFFL_{nd} is larger, and such solutions are more widely distributed in different heterogeneities. For four baselines, the changes in the values of their two indicators under the three levels of heterogeneity are relatively small. It is worth noting that PraFFL is robust to large-scale user

Table 3: Comparison of HV of algorithms under different number of clients on SYNTHETIC.

Method	The Number of Clients		
	3	10	20
LFT+Ensemble	0.479	0.478	0.473
LFT+Fedavg	0.698	0.641	0.589
Agnosticfair	0.530	0.559	0.555
FairFed	0.342	0.319	0.324
FedFB	0.599	0.594	0.599
PraFFL (Ours)	0.763	0.798	0.761

preferences. In other words, PraFFL not only have considerable performance in meeting users' dynamic preferences, but also maintain high stability under different degrees of data heterogeneity.

A.3.3 The difference between loss functions and metrics. Since the error rate and DP disparity are both non-differentiable functions,

the two loss functions (Eq. (1) and Eq. (3)) we used in the experiment are approximations of the error rate and DP disparity. To explore the gap between loss functions and indicators, we compare the Pareto front of the loss function value and the Pareto front of the indicator value on three real-world datasets in Fig. 10. We can find that PraFFL can obtain a better Pareto front for the two optimization objectives (loss functions). This shows that our proposed PraFFL has the ability to obtain high-quality Pareto front of optimized two objectives. For the Pareto front of the two metrics, we find that their distribution is sparse compared to the Pareto front of the loss function. This is a reasonable phenomenon because the two loss functions are approximations of the two indicators and they are not equivalent. The gap between the metrics and the loss function also exists in the experiments of the five baselines because it is affected by the functional nature of the metrics.